Modelling of Knudsen Layer Effects in Gaseous Couette Flows

Shashank Jaiswal · Nishanth Dongari (✉) · Vijay Kumar Saraswat
Department of Mechanical & Aerospace Engineering
Indian Institute of Technology Hyderabad
email: nishanth@iith.ac.in

Submitted to :

Submitted : 08 th March, 2016

Abstract

We investigate micro-scale Couette gas flows in the slip and transition flow regimes by incorporating Knudsen layer effects along with the modified second-order velocity slip and temperature jump boundary conditions. We have tested our approach with low and high Mach number velocity-driven (Couette) flow cases, and temperature-driven (Fourier heat transfer) flows. Our model shows excellent agreement with the direct simulation Monte-Carlo (DSMC) and kinetic theory models, thereby capturing the non-linear effects in the near wall region. On contrary, the conventional slip model results significantly overpredict the flow parameters and fails to capture the non-linear behaviour observed in the Knudsen layer. The results show that our approach greatly improves the near-wall accuracy of the Navier-Stokes-Fourier equations for modelling microscale gas flows, well beyond the slip-flow regime. The Knudsen layer model predicts smaller velocity slip, temperature jump and shear stress, which are caused by the shear-thinning property of the non-linear constitutive model, that is, vanishing effective viscosity in the transition flow regime. The importance of this paper also stems from the numerical simulation of non-equilibrium gas flows, as the implementation of the Knudsen layer modelling approach have been carried out in an open source CFD toolbox (OpenFOAM) which is capable of computing flows involving complex geometries.

Keywords : Non-linear Constitutive relations, Knudsen Layer, Couette flows, OpenFOAM

Nomenclature :-

Kn	Knudsen Number
Pr	Prandtl Number
p	Pressure (Pa)
U	Velocity (m/s)
T	Temperature (K)
Ma	Mach number
H	Distance between parallel plates
m	Molecular mass (kg)
tr	trace
I	Identity tensor
S	Transformation tensor
v	Boundary patch normal
R	Specific gas constant
A_s	First Sutherland coefficient (kg/(s.m.$K^{1/2}$))
T_s	Second Sutherland coefficient (K)
∇	Gradient
∇_n	Gradient normal to boundary patch
γ	Specific heat ratio
λ	Unconfined gas mean free path
λ_{eff}	Effective gas mean free path
β_{PL}	Normalized effective mean free path for momentum transfer
$(\beta_{PL})_T$	Normalized effective mean free path for energy transfer
ρ	Density (kg/m^3)
μ	Dynamic viscosity (kg/ms)
μ_{eff}	Effective dynamic viscosity (kg/ms)
ψ	Compressibility (s^2/m^2)
κ	Thermal conductivity (W/mK)
κ_{eff}	Effective thermal conductivity (W/mK)
Π_{mc}	Curvature Effect
σ_v	Momentum accommodation coefficient
σ_t	Thermal accommodation coefficient

Super and Subscripts :-

w	wall
f	fluid
T	transpose
∞	freestream condition

1. Introduction :-

In micro/rarefied gas flows, the gas molecule wall-surface interactions lead to the formation of Knudsen layer (KL): a local thermodynamically non-equilibrium region extending $\sim O(\lambda)$ from the surface, where λ is the gas mean free path (MFP) [1]. The Knudsen number (Kn) is defined as λ/H, where H is the characteristic length. Since the gas molecule-surface collisions are more frequent than gas molecule-molecule collisions in the KL, the gas MFP will effectively be reduced in the KL. It is noticed that the classical constitutive relations of the Navier-Stokes-Fourier (N-S-F) equations fail to predict non-linear behavior in the KL and deviations are significant in the slip ($10^{-3} < Kn < 10^{-1}$) and transition flow regimes ($10^{-1} < Kn < 10$) [1,2]. The gases at the surface exhibit non-newtonian viscosity behavior [3,4]. Ideally, one can resort to solving the Boltzmann equations [1,5–8] and carry out direct simulation Monte-Carlo (DSMC) simulations [2,9–11] to provide accurate predictions in the KL region. However, these methods are computationally intensive for low-speed flows in the slip and transition-flow regime, and large scale 3-D complex geometries.

The use of Maxwell velocity-slip [12] and subsequent modifications have been proposed to predict the velocity slip at the wall, which has led to second and higher order treatments of the non-equilibrium boundary conditions at the wall [13–16]. Recent review on available slip models of gas micro-flows [17] convey that the higher order slip and jump boundary conditions along with the conventional N-S-F equations provide better predictions for the integral flow parameters like mass flow rates, in the slip and transition flow regimes. However, such approaches fail to predict the non-linear flow behavior observed in the Knudsen layer [1,5–8].

Alternatively, geometry dependent effective mean free path [5,18–24] models are incor-

porated to extend the applicability of the N-S-F equations in the KL region. Guo et al. [18] suggests an extension of N-S-F equations to larger Kn by incorporating the gas molecular interactions with the boundary walls through modification of the classical expression of the MFP. Using a similar approach, Arlemark et al. [22] captured Poiseuille velocity flow profiles and the Poiseuille mass flow rate in planar geometries. Recently, Myong et al. [25] established the theoretical foundation for Couette flows in Knudsen regime using the non-linear coupled constitutive relations in continuum framework. These approaches have produced good results when compared with molecular-dynamics (MD) and DSMC data for various rarefied gas flow problems [18, 19, 21–23]. The computational costs of such approaches are negligible when compared to MD, DSMC and Boltzmann simulations.

The molecular dynamics (MD) simulations carried out by Dongari et al. [23, 26] indicate that the free paths of gas molecules follow a power-law (PL) probability distribution. The authors then accordingly hypothesized that the probability distribution function for the MFP of a rarefied gas followed a PL form, which is validated against MD data under various rarefied conditions. Using a PL distribution to describe free paths, Dongari et al. [21, 23, 27, 28] derived effective MFP models for flows confined by planar and non-planar surfaces, by taking into account the solid boundary effects. While the classical exponential MFP scaling approaches [19, 22] are limited up to $Kn \sim 0.2$, power-law based effective MFP models exhibit good agreement with the MD data up to the early transition regime ($Kn \sim 1$). Subsequently, the N-S-F constitutive relations, and the slip and jump boundary conditions are modified using the PL-based MFP scaling which accurately captured several non-equilibrium effects in the Knudsen layer.

Hence, in the current paper we implement the PL-based MFP approach to modify the classical constitutive relations and the boundary conditions in an open source CFD package OpenFOAM®. OpenFOAM [29, 30], based on C++ programming language [31], is capable of solving partial differential equations on unstructured meshes in parallel (using OpenMPI). The PL-based MFP scaling is incorporated in a density-based compressible solver *rhoCentralFoam* using our newly created thermo-physical model (named as *klPlanar*), and the new velocity

slip and temperature jump boundary conditions. We have rigorously tested our solver results against DSMC data and kinetic theory models for planar geometries. The test cases include subsonic and transonic Couette flow and Fourier heat transfer between parallel plates, covering both the slip and transition flow regimes, thereby testing both the Mach number and Knudsen number dependence of the non-linear velocity profile [32].

2. Numerical Simulations :-

The OpenFOAM [29,30] (Open Field Operation and Manipulation) CFD Toolbox is a free and open source CFD software package which has an extensive range of features to solve complex fluid flow problems for arbitrary structured and unstructured grids. OpenFOAM is primarily written in the object oriented programming language C++ [31]. It makes heavy use of the concepts of C++ templates, function and operator overloading [29]. The primary solvers (including meshing, and pre-processing and post-processing) run in parallel using the method of domain decomposition and Massage Passing Interface (MPI) between processes on host, enabling the users to take full advantage of host computer.

A second order accurate central scheme (in terms of numerical viscosity $\sim O(\triangle x^{2r-1})$) has been recently proposed by Kurganov and Tadmor [33], and consequently the authors proposed the semi-discrete central scheme formulation [34] as the second order generalization of the celebrated Lax-Friedrichs scheme [33,35] for hyperbolic conservation laws. *rhoCentralFOAM* [35] is a density based compressible solver available in OpenFOAM, which implements the semi-discrete central scheme formulation as proposed by Kurganov and Tadmor [34]. The solver has the capability to simulate arbitrary 2D/3D geometries with a variety of boundary conditions (Dirichlet, Neumann or Robin). The solver has been benchmarked [35] and rigorously used for studying hypersonic [36], subsonic [37] and thermal [38,39] gas flow problems.

Therefore, *rhoCentralFoam* has been used in our current work for all the simulations. Since we deal with micrometer sized geometries and hence the Reynolds number is small (< 100), the test cases has been treated as laminar. The planar geometries enables us to use structured meshes for all the test cases. The meshes have been generated using the default mesh

generation utility (*blockMesh*) present in OpenFOAM.

3. Implementation Of Effective MFP :-

The geometry dependent effective MFP [18, 19, 21, 22] models have been incorporated to extend the applicability of the Navier-Stokes-Fourier equations in the KL region. The viscosity correction models based on wall function corrections have been already well established [21, 22, 40–43]. However, the implementation of such models in open source CFD frameworks such as OpenFOAM, relatively remains unexplored. We incorporate the effective MFP expression based on the power-law distribution function developed by Dongari et al. [21] for planar geometries.

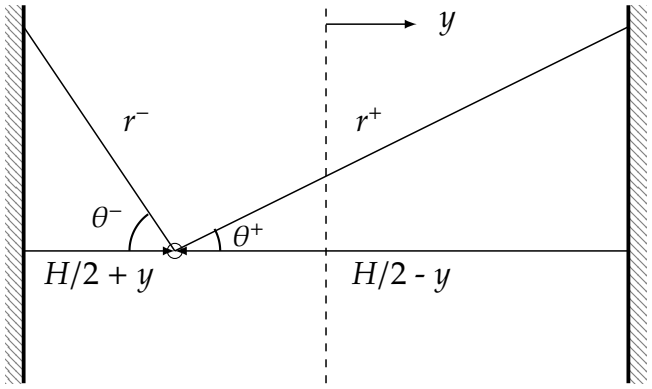

Figure 1: A molecule confined between two planar walls with spacing H The molecule has an equal probability to travel in any zenith angle θ^- or θ^+ or to travel in either the positive or negative y direction. The molecule under consideration is assumed to have just experienced an intermolecular collision at its current position $H/2 + y$. [21, 22]

Dongari et al. [21, 23] derived the power law based MFP model for the planar-wall configuration as shown in Fig. 1. A molecule is shown confined between the two parallel walls separated by a distance of H. The molecule has an equal probability to travel in any zenith angle θ^- or θ^+. The symbol r^- has been used for the molecule traveling in the negative y direction, and r^+ if the molecule is traveling in the positive y direction. (See [21, 22])

The power law (PL) based effective MFP can be expressed as :

$$\begin{aligned}\lambda_{\text{eff(PL)}} &= \frac{\lambda}{2}\left[p(r^-) + p(r^+)\right] \\ &= \lambda\left\{1 - \frac{1}{2}\left[\left(1 + \frac{r^-}{a}\right)^{1-n} + \left(1 + \frac{r^+}{a}\right)^{1-n}\right]\right\}\end{aligned} \tag{1}$$

where λ is unconfined gas mean free path, $p(r)$ is the power-law probability distribution function , $a = \lambda\ (n-2)$ and $n = 3$ unless otherwise explicitly stated [21,23,26,28].

A three-dimensional MFP can be obtained by averaging the free path with respect to θ^- and θ^+ in the range $[0, \pi/2]$ using the mean integral theorem as :

$$\left\langle \lambda_{\text{eff(PL)}}(\theta) \right\rangle = \frac{2}{\pi}\int_0^{\pi/2} \lambda_{\text{eff(PL)}}(\theta)d\theta \tag{2}$$

which upon averaging over free path using Simpson's numerical integration over 16 subintervals results in $\lambda_{\text{eff}} = \lambda\beta_{PL}$ [23], where

$$\begin{aligned}\beta_{\text{PL}} = 1 - \frac{1}{96}\Bigg[&\left(1 + \frac{H/2 - y}{a}\right)^{1-n} + \left(1 + \frac{H/2 + y}{a}\right)^{1-n} \\ &+4\sum_{i=1}^{8}\left(1 + \frac{H/2 - y}{acos[(2i-1)\pi/32]}\right)^{1-n} \\ &+4\sum_{i=1}^{8}\left(1 + \frac{H/2 + y}{acos[(2i-1)\pi/32]}\right)^{1-n} \\ &+2\sum_{i=1}^{7}\left(1 + \frac{H/2 - y}{acos[i\pi/16]}\right)^{1-n} \\ &+2\sum_{i=1}^{7}\left(1 + \frac{H/2 + y}{acos[i\pi/16]}\right)^{1-n}\Bigg]\end{aligned} \tag{3}$$

The unconfined MFP for energy transfer between molecules can be defined as $\lambda_{\text{T}} = 1.922\lambda_{\text{HS}}$, where the subscript HS denotes hard-sphere molecules [1,21]. Therefore, the modified constant for thermal cases becomes :

$$a_{\text{T}} = \lambda_{\text{T}}\ (n-2) \tag{4}$$

Further, the normalized effective MFP for thermal Knudsen layer can be defined as $(\beta_{PL})_T$, which can be obtained by replacing a with a_T in Eq. (3).

Thus, the effective transport properties can be expressed as:

$$\mu_{eff} = \mu(T)\ \beta_{PL} \tag{5}$$

$$\kappa_{eff} = \kappa(T)\ (\beta_{PL})_T \tag{6}$$

where μ is non-constant viscosity, μ_{eff} is *effective viscosity*, κ is thermal conductivity, and κ_{eff} is *effective thermal conductivity*.

In the Fig. 2, grids represent a collocated two dimensional mesh where each small rectangular grid represents a cell. The scalar properties (for example : viscosity (μ)) are defined at cell centers. On such a grid, the effective MFP based transport property scaling can be described as given below.

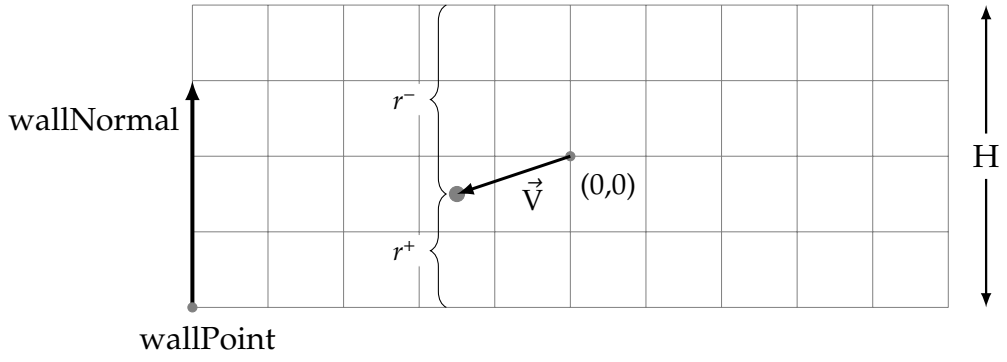

FIGURE 2: Schematic for computation of β_{PL} in a cell for a simple uniform grid.

Since μ is a scalar field defined on cell-centers of collocated mesh, the correction i.e. β_{PL} / $(\beta_{PL})_T$ is also defined as a scalar field on cell-centers of collocated mesh (Refer Fig. 2). For the purpose of calculating β_{PL} / $(\beta_{PL})_T$ in a particular cell, we take the cell centre coordinate of the cell and find it's wall normal distance corresponding to the two walls which is then substituted in the Eq. (3). Since the equation is symmetric, the order in which we substitute the wall normal distance values in the equation does not affect the computed β_{PL} value. As far as β_{PL} / $(\beta_{PL})_T$ values at zero-volume boundary patches are concerned, we take face-center

coordinate values and proceed with our calculation. Based upon the pre-existing template of thermo-physical models present in OpenFOAM, we have created a new set of thermo-physical model (named *klPlanar*), which takes into account the correction of transport properties based upon β_{PL} / $(\beta_{\mathrm{PL}})_{\mathrm{T}}$.

The modified N-S-F constitutive relation also needs to be solved in conjunction with the appropriate slip boundary conditions to capture the non-equilibrium phenomena in the KL [21]. OpenFOAM implements the Maxwell velocity slip and Smoluchowski temperature jump boundary conditions in the *rhoCentralFoam* solver [35]. The current implementation of Maxwell velocity slip and Smoluchowski temperature jump in OpenFOAM can be mathematically expressed as [35,38,44]:

$$U = U_w - \frac{2-\sigma_v}{\sigma_v}\lambda\nabla_n(S.U) - \frac{2-\sigma_v}{\sigma_v}\frac{\lambda}{\mu}S.(v.\Pi_{mc}) - \frac{3}{4}\frac{\mu}{\rho}\frac{S.\nabla T}{T} \tag{7}$$

$$T = T_w - \frac{2-\sigma_t}{\sigma_t}\frac{2\gamma}{(\gamma+1)Pr}\lambda(v.\nabla T) \tag{8}$$

respectively, with,

$$\frac{\lambda}{\mu} = \sqrt{\frac{\pi\psi}{2}}\frac{1}{\rho} \tag{9}$$

$$\Pi_{mc} = \mu(\nabla U)^T - (2/3)Itr(\nabla U) \tag{10}$$

where σ_v is the tangential momentum accommodation coefficient, σ_t is the thermal accommodation coefficient, U_w is wall velocity, T_w is wall temperature, v is the boundary patch normal,Pr is Prandtl number, γ is adiabatic index, and $S = I\text{-}v * v$ is the identity tensor which removes normal components of any nonscalar field, eg. velocity, so that slip occurs in the direction tangential to surface. Four terms that appear on right side of Eq. (7) correspond to wall velocity, effects of viscous stresses, it's curvature effect and thermal creep, respectively.

For our planar geometry, effect of the curvature term can be neglected. Hence, Eq. (7)

using (9) can be simplified to:

$$U = U_w - \frac{2-\sigma_v}{\sigma_v}\sqrt{\frac{\pi\psi}{2}}\frac{\mu}{\rho}\nabla_n(S.U) - \frac{3}{4}\frac{\mu}{\rho}\frac{S.\nabla T}{T} \tag{11}$$

Using Eqs. (6) and (5), the modified velocity slip boundary condition can be expressed as :

$$U = U_w - \frac{2-\sigma_v}{\sigma_v}\sqrt{\frac{\pi\psi}{2}}\frac{\mu\beta_{\mathrm{PL}}}{\rho}\nabla_n(S.U) - \frac{3}{4}\frac{\mu\ (\beta_{\mathrm{PL}})_{\mathrm{T}}}{\rho}\frac{S.\nabla T}{T} \tag{12}$$

In similar manner, using Eqs. (8) and (9), the Smolouchowski temperature jump boundary condition for planar geometries can be expressed as:

$$T = T_w - \frac{2-\sigma_t}{\sigma_t}\frac{2\gamma}{(\gamma+1)Pr}\sqrt{\frac{\pi\psi}{2}}\frac{\mu}{\rho}(v.\nabla T) \tag{13}$$

Using Eq. (5), the modified temperature jump boundary condition can be expressed as:

$$T = T_w - \frac{2-\sigma_t}{\sigma_t}\frac{2\gamma}{(\gamma+1)Pr}\sqrt{\frac{\pi\psi}{2}}\frac{\mu\ (\beta_{\mathrm{PL}})_{\mathrm{T}}}{\rho}(v.\nabla T) \tag{14}$$

It is to be noted that the coefficients appearing in the velocity & jump boundary conditions are no more constant. Using these new nonlinear coupled velocity slip and temperature jump models, a seamless combination of two nonlinearities and couplings – Effective transport properties for bulk flow and nonlinear coupled boundary conditions at the wall– can be achieved. It must be emphasized that similar heuristic boundary conditions have been proposed in past (See Guo et al. [18]), and more recently by Myong et al. [25].

4. Test Cases :-

The incorporation of Knudsen layer effects into the *rhoCentralFoam* solver has been tested for various flow configurations with planar geometries. For all the test cases, the accommodation coefficients σ_t and σ_v are assigned a value of unity; i.e. fully diffuse reflection has been

assumed for all walls. The viscosity is obtained from Sutherland's model, and it's coefficients for Argon are $R = 208\ J/(kg.K)$, $T_s = 144$ K and $A_s = 1.96\times10^{-6}$ kg/(s.m.K$^{1/2}$) [45]. Unless otherwise explicitly stated, these conditions remain the same throughout the paper. The N-S-F equations with the conventional slip/jump conditions (Eqs. 11 and 13) based results are referred as "*Conventional slip model*", while the results with the Knudsen layer effects (Eqs. 12 and 14) are denoted as "*Knudsen layer model*".

4.1. Subsonic Couette Flow :-

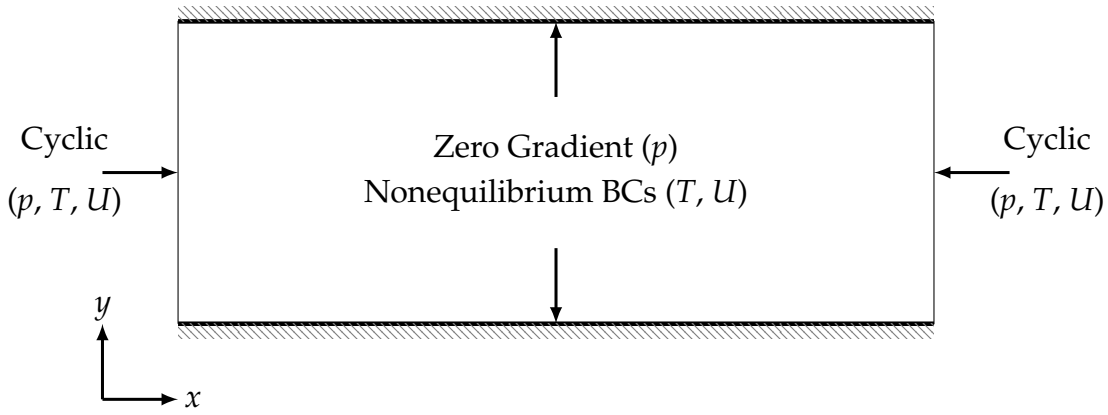

FIGURE 3: Numerical setup for a simple Couette flow case

4.1.1. Case-1 :-

For this test case, the coordinates are chosen such that the walls are parallel to the x direction and y is the direction perpendicular to the plates. The schematic as well as boundary conditions applied at boundary patches have been shown in Fig.3. The two parallel plates have been set at $y = \pm H/2$, where upper and lower plates move with a constant velocity $U_w = \pm 50\ ms^{-1}$. The external accelerations are set to as $a_x = a_y = 0$ and the wall temperature is fixed at $T_w = 273$ K.

Figure (4) demonstrates normalized velocity profiles for $Kn = 0.5$ and 1.0. The results obtained from *conventional slip model* and *knudsen layer model* have been compared with the DSMC data. Our *knudsen layer model* is in fair agreement with the DSMC data [45], where both predict non-linear nature of velocity profile in the near wall region, i.e Knudsen layer.

However, the *conventional slip model* fail to exhibit this behavior, and for both Knudsen numbers, the *conventional slip model* over-predicts the amount of velocity slip ($\sim$ 12% and $\sim$ 26% for $Kn = 0.5$ and 1.0 respectively). The *knudsen layer model* not only predicts the correct velocity slip at the wall but also the power-law behavior of velocity profile [3,21,23] in Knudsen layer even in the transition flow regime.

4.1.2. Case-2 :-

In the previous test case, we have demonstrated the non-linear nature of the velocity profile in the Knudsen layer. In the current case, we demonstrate the near-wall accuracy of our *knudsen layer model* as a function of Kn. For this test case, the geometrical setup is same as Case-1. The upper and lower plates move with a constant velocity $U_w = \mp\, 0.5\, C_s\, ms^{-1}$, where $C_s = \sqrt{\gamma RT}$, i.e. Mach number of ∓ 0.5, where $Ma = U/C_s$. The external accelerations are set to as $a_x = a_y = 0$ and the wall temperature is fixed at $T_w = 273$ K.

In Fig. 5, we present the normalized velocity slip values as a function of Knudsen number covering the slip and transition flow regimes. Results from our *knudsen layer model* exhibit excellent agreement with the DSMC and Boltzmann-BGK data [8,46]. We have also demonstrated *conventional slip model* and Lattice-Boltzmann simulations. Both the D2Q9 and *conventional slip model* results significantly over-predict the slip velocities, while the D2Q16 is able to accurately capture the velocity slip. At $Kn = 1.5$, the deviation between *conventional slip model* and *knudsen layer model* is $\sim$ 26%. The Knudsen layer model is as accurate as higher-order Lattice Boltzmann technique (D2Q16) without incurring any additional computational resources.

4.2. Transonic Couette Flow :-

4.2.1. Case-1 :-

We further explore the Knudsen layer effects for flows in the transonic regime. For this test case, the coordinates are chosen such that the walls are parallel to the x-direction and y is the direction perpendicular to the plates. The two parallel plates have been set at $y = 0$ and $y = H$. The upper remains stationary while the lower wall moves with a constant velocity of $\sqrt{RT}$ (Ma $\sim$ 0.8). The external acceleration are set to as $a_x = a_y = 0$. The wall temperature is fixed at

$T_w = 273$ K.

In the Fig. 6, the normalized velocity profiles (across the channel height) obtained with the *knudsen layer model* and *conventional slip model* have been compared with the DSMC data for $Kn = 0.5$ and 1.0 [47]. For $Ma \sim 0.8$ as well, our *knudsen layer model* is in excellent agreement with the DSMC solution for both Knudsen numbers, whereas the *conventional slip model* over-predicts the velocity slip in near-wall region ($\sim 14\%$ and $\sim 16.5\%$ for $Kn = 0.5$ and 1.0 respectively).

4.2.2. Case-2 :-

In the previous test case, we have demonstrated the velocity profile in the Knudsen layer. In the current case, we demonstrate the accuracy of our *knudsen layer model* for temperature jump predictions as a function of Kn. For this test case, the geometrical setup is same as Case-1. The upper and lower plates move with a constant velocity $U_w = \mp\, 0.8\, C_s\ ms^{-1}$, where $C_s = \sqrt{\gamma RT}$, i.e. Mach number of ∓ 0.8, where $Ma = U/C_s$. The external accelerations are set to as $a_x = a_y = 0$ and the wall temperature is fixed at $T_w = 273$ K.

In Fig. 7, we present the normalized temperature jump values as a function of Knudsen number covering the slip and transition flow regimes. Results from our *knudsen layer model* exhibit good agreement with the DSMC and Boltzmann simulations [25]. *conventional slip model* results significantly under-predict the temperature jump, while the *knudsen layer model* is able to fairly capture the jump, if not exactly precise.

4.3. Fourier Heat Transfer :-

Earlier test cases dealt with velocity driven flows, where we have demonstrated the accuracy of Knudsen layer modeling of momentum equations. Here, we showcase the accuracy of thermal Knudsen layer modeling of energy equation by solving the Fourier heat transfer problem. For this test case, the geometrical setup is same as in case of transonic Couette Flow, where the upper and lower walls remain stationary. The lower wall i.e, cold junction

temperature is fixed at T_w = 263 K while the upper wall i.e, hot junction temperature is fixed at 283K. The reference temperature i.e. T_{ref}, is 273 K

Figure 8 shows the normalized temperature variation along the cross-section for $Kn = 0.475$ and $Kn = 1.58$ [48], where we compare our *knudsen layer model* results with the DSMC data. For both Knudsen numbers, *knudsen layer model* results are in fair agreement with the DSMC data, although minor deviations are noticed at the wall. Non-linear temperature profiles are exhibited due to the presence of thermal Knudsen layer and the *conventional slip model* over-predicts the temperature ($\sim 1\%$ and $\sim 2\%$ for $Kn = 0.475$ and 1.58 respectively).

5. Conclusions :-

We have modelled the Knudsen layer flow behavior using the power-law based constitutive scaling approach. The implementation has been carried out within an open source computational fluid dynamics framework OpenFOAM. The modelling implementation has been tested for the cases of subsonic and transonic Couette gas flows, and Fourier heat transfer.

The current modelling captures many of the trends associated with the complex nonequilibrium physics of the Knudsen layer. Our results exibit excellent agreement with DSMC data in both the Knudsen layer and bulk flow regions up to $Kn \sim 1$. Hence, with current approach, we can improve the predictive capabilities of the N-S-F framework into the transition flow regime and indeed for rarefied high speed gas flows as well.

The major importance of this paper stems from the fact that the Knudsen layer implementation is carried out in an open-source CFD software and indeed with the additional computational cost to be negligible. The tool can be applied to test complex geometries involving structured and unstructured grids. Further advantages include parallel computing abilities and extension of existing functionalities (for example: see [10,35]) to incorporate new models with better accuracy in the future.

The present results may also motivate future work into understanding the origin of non-

equilibrium physics in rarefied gases, including:

- Incorporating modified higher-order slip and jump boundary conditions [2,13,14,49,50].
- The implementation of Knudsen layer modeling for non-planar and complex geometries [27,28].
- Extending the applicability of Knudsen layer implementation for wide range of supersonic/hypersonic test cases including the turbulence modeling.

6. Acknowledgments :-

The research leading to these results has received funding from the Department of Science and Technology (DST) India under the INSPIRE Faculty Award. The author VKS would like to thank Department of Atomic Energy (DAE) India for support through Homi Bhabha Chair at IIT Hyderabad.

References :-

[1] Sone, Y. *Kinetic theory and fluid dynamics*. Springer Science & Business Media, 2002.

[2] Karniadakis, G., Beskok, A., and Aluru, N. *Microflows and nanoflows: fundamentals and simulation*, vol. 29. Springer Science & Business Media, 2006.

[3] Lilley, C. R., and Sader, J. E. Velocity gradient singularity and structure of the velocity profile in the knudsen layer according to the boltzmann equation. *Physical Review E 76*, 2 (2007), 026315.

[4] Garzó, V., and Santos, A. *Kinetic Theory of Gases in Shear Flows: Nonlinear Transport*, vol. 131. Springer Science & Business Media, 2003.

[5] Cercignani, C. *The Boltzmann equation*. Springer, 1988.

[6] Chen, S., and Doolen, G. D. Lattice boltzmann method for fluid flows. *Annual review of fluid mechanics 30*, 1 (1998), 329–364.

[7] Ansumali, S., and Karlin, I. V. Kinetic boundary conditions in the lattice boltzmann method. *Physical Review E 66*, 2 (2002), 026311.

[8] Ansumali, S., Karlin, I., Arcidiacono, S., Abbas, A., and Prasianakis, N. Hydrodynamics beyond navier-stokes: Exact solution to the lattice boltzmann hierarchy. *Physical review letters 98*, 12 (2007), 124502.

[9] Bird, G. A. Molecular gas dynamics and the direct simulation of gas flows.

[10] Scanlon, T., Roohi, E., White, C., Darbandi, M., and Reese, J. An open source, parallel dsmc code for rarefied gas flows in arbitrary geometries. *Computers & Fluids 39*, 10 (2010), 2078–2089.

[11] Oran, E., Oh, C., and Cybyk, B. Direct simulation monte carlo: recent advances and applications 1. *Annual Review of Fluid Mechanics 30*, 1 (1998), 403–441.

[12] Maxwell, J. C. On stresses in rarified gases arising from inequalities of temperature. *Philosophical Transactions of the royal society of London* (1879), 231–256.

[13] Deissler, R. An analysis of second-order slip flow and temperature-jump boundary conditions for rarefied gases. *International Journal of Heat and Mass Transfer 7*, 6 (1964), 681–694.

[14] Cercignani, C. Higher order slip according to the linearized boltzmann equation. Tech. rep., DTIC Document, 1964.

[15] Beskok, A. Validation of a new velocity-slip model for separated gas microflows. *Numerical Heat Transfer: Part B: Fundamentals 40*, 6 (2001), 451–471.

[16] Barber, R. W., and Emerson, D. R. Challenges in modeling gas-phase flow in microchannels: from slip to transition. *Heat Transfer Engineering 27*, 4 (2006), 3–12.

[17] Zhang, W.-M., Meng, G., and Wei, X. A review on slip models for gas microflows. *Microfluidics and nanofluidics 13*, 6 (2012), 845–882.

[18] Guo, Z., Shi, B., and Zheng, C. G. An extended navier-stokes formulation for gas flows in the knudsen layer near a wall. *Europhysics Letters 80*, 2 (2007), 24001.

[19] Stops, D. The mean free path of gas molecules in the transition regime. *Journal of Physics D: Applied Physics 3*, 5 (1970), 685.

[20] Lockerby, D. A., and Reese, J. M. On the modelling of isothermal gas flows at the microscale. *Journal of Fluid Mechanics 604* (2008), 235–261.

[21] Dongari, N., Zhang, Y., and Reese, J. M. Modeling of knudsen layer effects in micro/nanoscale gas flows. *Journal of Fluids Engineering 133*, 7 (2011), 071101.

[22] Arlemark, E. J., Dadzie, S. K., and Reese, J. M. An extension to the navier–stokes equations to incorporate gas molecular collisions with boundaries. *Journal of Heat Transfer 132*, 4 (2010), 041006.

[23] Dongari, N., Zhang, Y., and Reese, J. M. Molecular free path distribution in rarefied gases. *Journal of Physics D: Applied Physics 44*, 12 (2011), 125502.

[24] Zhang, Y.-H., Gu, X.-J., Barber, R. W., and Emerson, D. R. Capturing knudsen layer phenomena using a lattice boltzmann model. *Physical Review E 74*, 4 (2006), 046704.

[25] Myong, R. S. Theoretical description of the gaseous knudsen layer in couette flow based on the second-order constitutive and slip-jump models. *Physics of Fluids 28*, 1 (2016).

[26] Dongari, N. *Micro Gas Flows: Modelling the Dynamics of Knudsen Layers*. University of Strathclyde, 2012.

[27] Dongari, N., Barber, R. W., Emerson, D. R., Stefanov, S. K., Zhang, Y., and Reese, J. M. The effect of knudsen layers on rarefied cylindrical couette gas flows. *Microfluidics and nanofluidics 14*, 1-2 (2013), 31–43.

[28] Dongari, N., White, C., Scanlon, T. J., Zhang, Y., and Reese, J. M. Effects of curvature on rarefied gas flows between rotating concentric cylinders. *Physics of Fluids (1994-present) 25*, 5 (2013), 052003.

[29] Weller, H. G., Tabor, G., Jasak, H., and Fureby, C. A tensorial approach to computational continuum mechanics using object-oriented techniques. *Computers in physics 12*, 6 (1998), 620–631.

[30] Jasak, H., Jemcov, A., and Tukovic, Z. Openfoam: A c++ library for complex physics simulations.

[31] Stroustrup, B. *The C++ programming language*. Pearson Education India, 1986.

[32] Myong, R. S. On the high mach number shock structure singularity caused by overreach of maxwellian molecules. *Physics of Fluids 26*, 5 (2014).

[33] Kurganov, A., and Tadmor, E. New high-resolution central schemes for nonlinear conservation laws and convection–diffusion equations. *Journal of Computational Physics 160*, 1 (2000), 241–282.

[34] Kurganov, A., Noelle, S., and Petrova, G. Semidiscrete central-upwind schemes for hyperbolic conservation laws and hamilton–jacobi equations. *SIAM Journal on Scientific Computing 23*, 3 (2001), 707–740.

[35] Greenshields, C. J., Weller, H. G., Gasparini, L., and Reese, J. M. Implementation of semi-discrete, non-staggered central schemes in a colocated, polyhedral, finite volume framework, for high-speed viscous flows. *International journal for numerical methods in fluids 63*, 1 (2010), 1–21.

[36] Greenshields, C. J., and Reese, J. M. Rarefied hypersonic flow simulations using the navier–stokes equations with non-equilibrium boundary conditions. *Progress in Aerospace Sciences 52* (2012), 80–87.

[37] Bohorquez, P., and Parras, L. Three-dimensional numerical simulation of the wake flow of an afterbody at subsonic speeds. *Theoretical and Computational Fluid Dynamics 27*, 1-2 (2013), 201–218.

[38] Mohammadzadeh, A., Roohi, E., Niazmand, H., Stefanov, S., and Myong, R. S. Thermal and second-law analysis of a micro-or nanocavity using direct-simulation monte carlo. *Physical Review E 85*, 5 (2012), 056310.

[39] Le, N. T., White, C., Reese, J. M., and Myong, R. S. Langmuir–maxwell and langmuir–smoluchowski boundary conditions for thermal gas flow simulations in hypersonic aerodynamics. *International Journal of Heat and Mass Transfer 55*, 19 (2012), 5032–5043.

[40] Lockerby, D. A., Reese, J. M., and Gallis, M. A. Capturing the knudsen layer in continuum-fluid models of nonequilibrium gas flows. *AIAA journal 43*, 6 (2005), 1391–1393.

[41] Fichman, M., and Hetsroni, G. Viscosity and slip velocity in gas flow in microchannels. *Physics of Fluids (1994-present) 17*, 12 (2005), 123102.

[42] Bahukudumbi, P. A unified engineering model for steady and quasi-steady shear-driven gas microflows. *Microscale Thermophysical Engineering 7*, 4 (2003), 291–315.

[43] Mizzi, S., Barber, R., Emerson, D., Reese, J., and Stefanov, S. A phenomenological and extended continuum approach for modelling non-equilibrium flows. *Continuum Mechanics and Thermodynamics 19*, 5 (2007), 273–283.

[44] Le, N., Greenshields, C. J., and Reese, J. Evaluation of nonequilibrium boundary conditions for hypersonic rarefied gas flows. In *Progress in Flight Physics* (2012), vol. 3, EDP Sciences, pp. 217–230.

[45] Gu, X.-j., and Emerson, D. R. A high-order moment approach for capturing non-equilibrium phenomena in the transition regime. *Journal of Fluid Mechanics 636* (2009), 177–216.

[46] Willis, D. R. Comparison of kinetic theory analyses of linearized couette flow. *Physics of Fluids (1958-1988) 5*, 2 (1962), 127–135.

[47] Xue, H., and Ji, H. Prediction of flow and heat transfer characteristics in micro-couette flow. *Microscale Thermophysical Engineering 7*, 1 (2003), 51–68.

[48] Gallis, M., Rader, D., and Torczynski, J. Calculations of the near-wall thermophoretic force in rarefied gas flow. *Physics of Fluids (1994-present) 14*, 12 (2002), 4290–4301.

[49] Guo, Z., Qin, J., and Zheng, C. Generalized second-order slip boundary condition for nonequilibrium gas flows. *Physical Review E 89*, 1 (2014), 013021.

[50] Rooholghdos, S. A., and Roohi, E. Extension of a second order velocity slip/temperature jump boundary condition to simulate high speed micro/nanoflows. *Computers & Mathematics with Applications 67*, 11 (2014), 2029–2040.

(a) Normalized velocity profile for $Kn = 0.5$

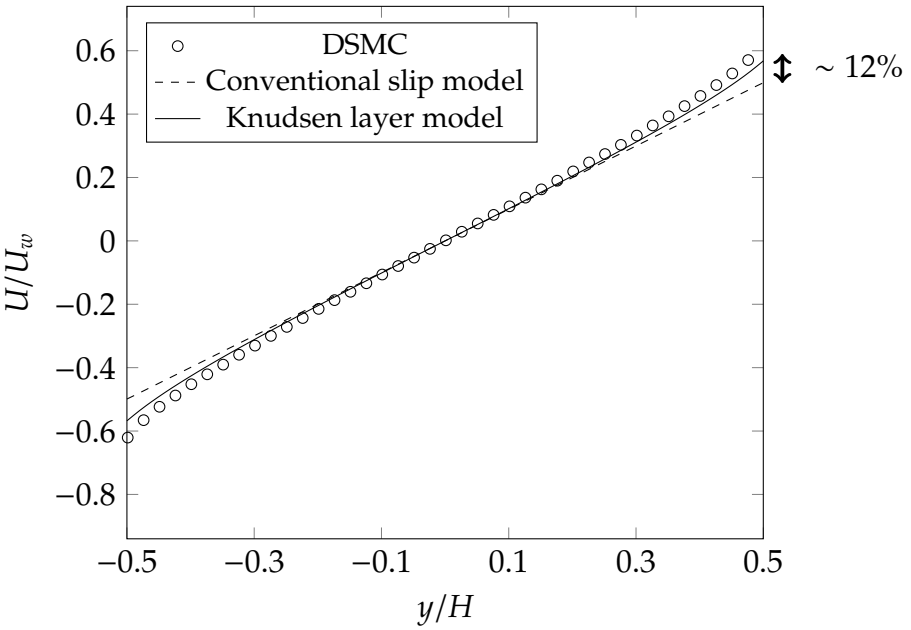

(b) Normalized velocity profile for $Kn = 1.0$

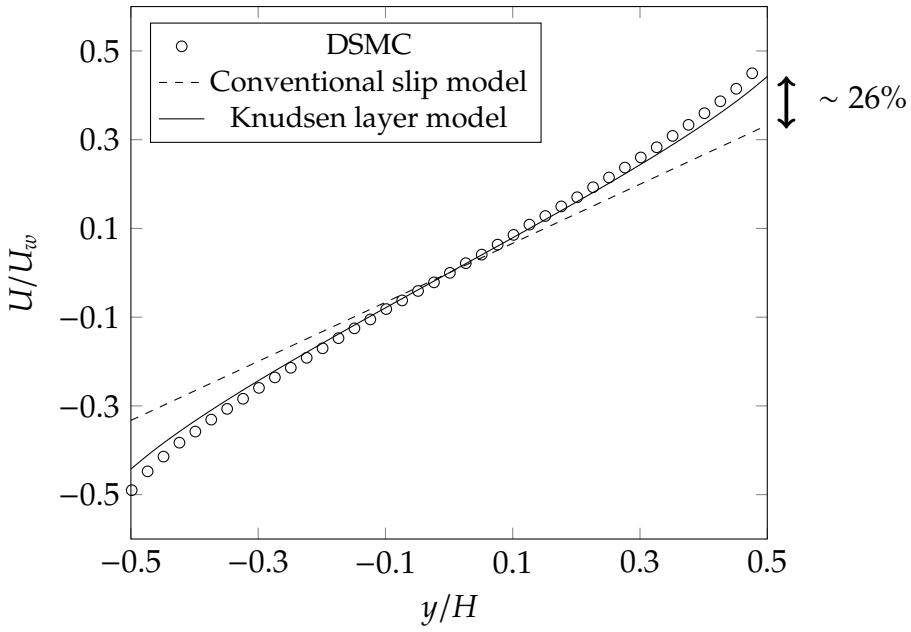

FIGURE 4: Normalized velocity profiles in subsonic micro-channel Couette flow under rarefied conditions: (a) $Kn = 0.5$ and (b) $Kn = 1.0$. Knudsen layer model results are compared against DSMC data [45] and the *conventional slip model* .

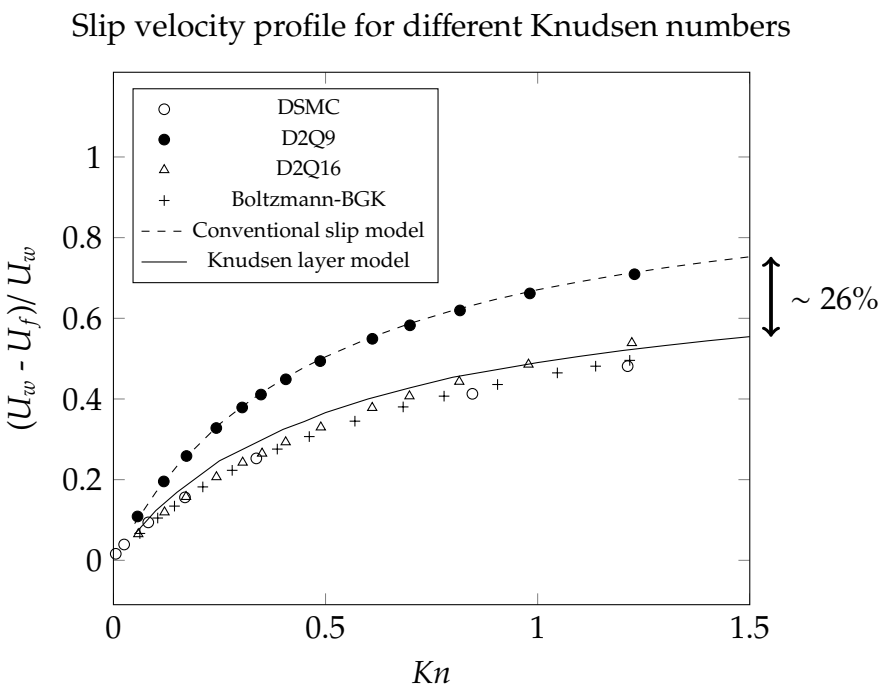

FIGURE 5: Wall-Normalized slip velocity variation as a function of Knudsen number for a subsonic micro-channel Couette flow test case. Knudsen layer model results are compared against DSMC and other kinetic theory models [8, 46].

(a) Normalized velocity profile for $Kn = 0.5$

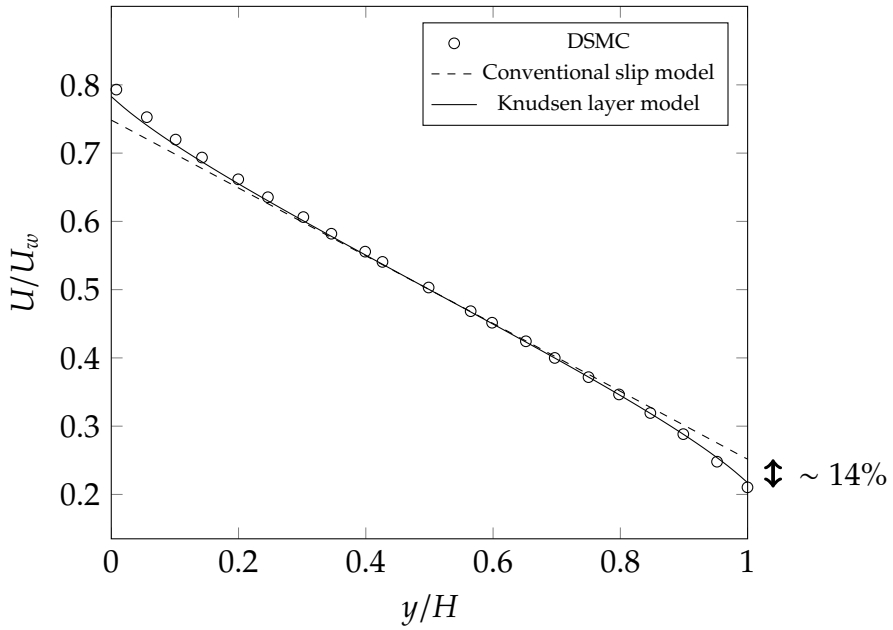

(b) Normalized velocity profile for $Kn = 1$

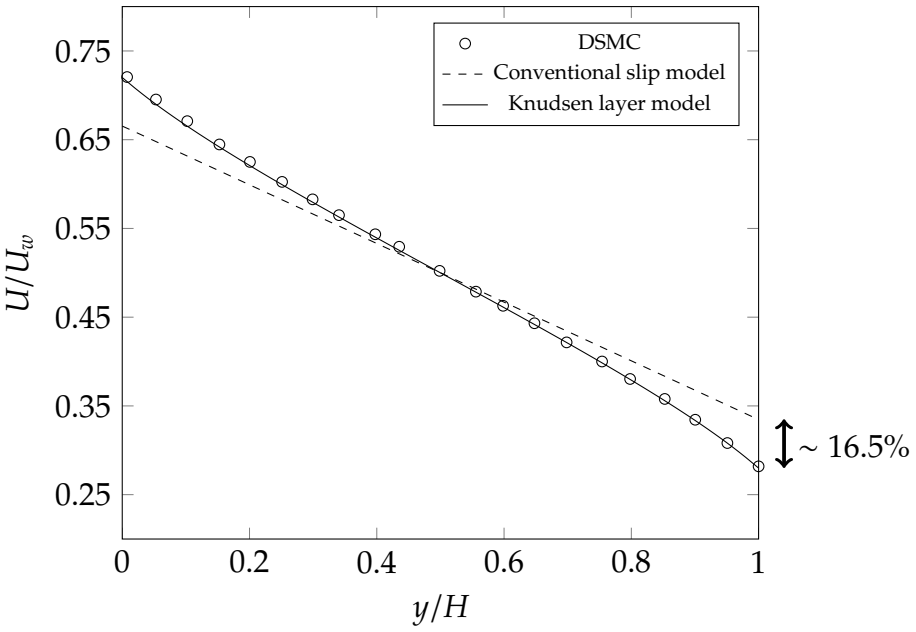

FIGURE 6: Normalized velocity profiles in transonic micro-channel Couette flow under rarefied conditions: (a) $Kn = 0.5$ and (b) $Kn = 1.0$. Knudsen layer model results are compared against DSMC data [47] and the *conventional slip model* .

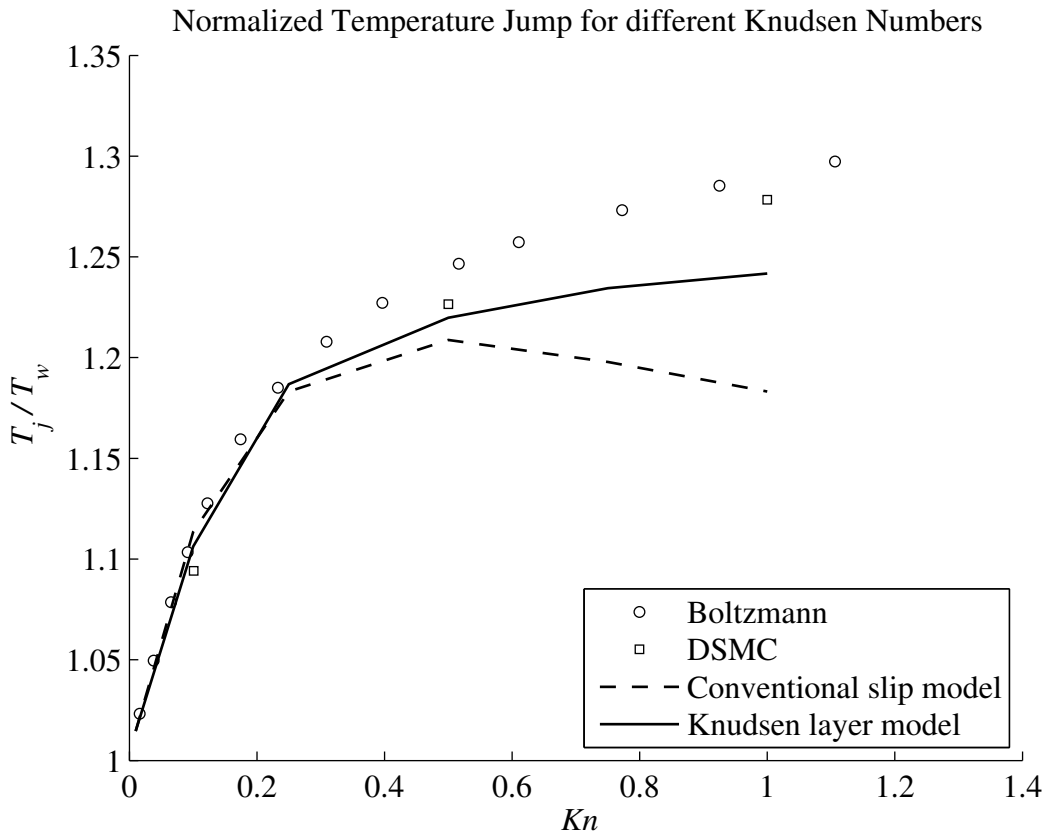

FIGURE 7: Wall-Normalized temperature jump variation as a function of Knudsen number for a transonic micro-channel Couette flow test case. Knudsen layer model results are compared against DSMC and other kinetic theory models [25].

(a) Normalized temperature profile for $Kn = 0.475$

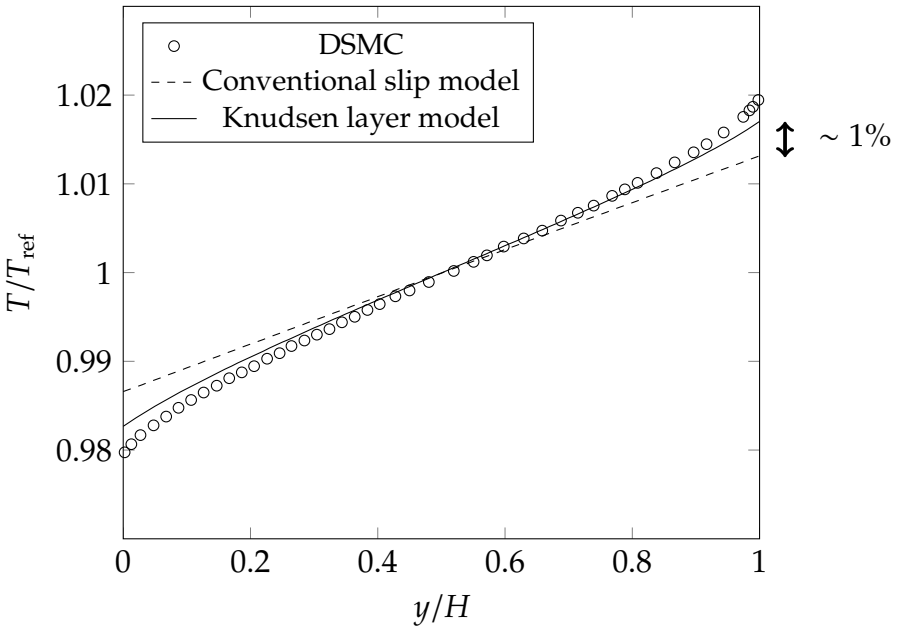

(b) Normalized temperature profile for $Kn = 1.58$

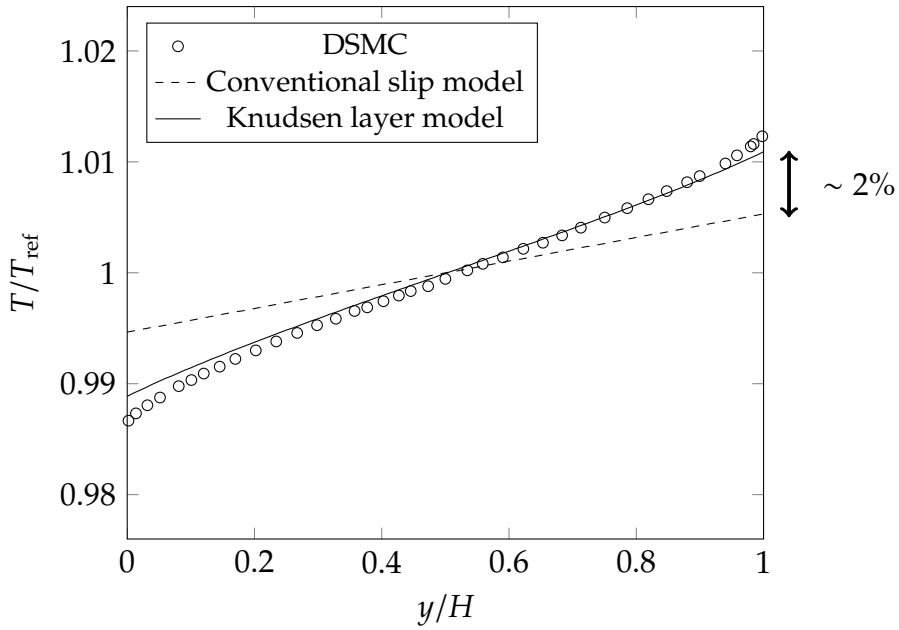

FIGURE 8: Normalized temperature profiles in micro-channel Fourier heat transfer under rarefied conditions: (a) $Kn = 0.475$ and (b) $Kn = 1.58$. Knudsen layer model results are compared against DSMC data [48] and the *conventional slip model* .